PHYSICAL REVIEW LETTERS

Molecular Orientation and Alignment by Intense Single-Cycle THz Pulses

Sharly Fleischer, Yan Zhou, Robert W. Field, and Keith A. Nelson

Department of Chemistry, Massachusetts Institute of Technology, Cambridge, Massachusetts 02139

Intense single-cycle THz pulses resonantly interacting with molecular rotations are shown to induce field-free orientation and alignment under ambient conditions. We calculate and measure the degree of both orientation and alignment induced by the THz field in an OCS gas sample, and correlate between the two observables. The data presents the first observation of THz-induced molecular alignment in the gas phase.

In amorphous media such as gases and liquids, most spectroscopic signatures are averaged over all molecular orientations, owing to the isotropic angular distribution at the instant of measurement. Since in most light-matter processes, the interaction between the field and a molecule depends on the projection of the field polarization axis onto the body-fixed transition dipole moment (whether permanent or induced), preparation of a molecular sample with well defined angular distribution prior to its further interrogation is beneficial in terms of efficiency, selectivity, and resolution, owing to the removal or reduction of angular averaging. This has motivated the development of "laser induced molecular alignment", a very active field of research in the last two decades, in which gas-phase molecules are rotationally excited by intense, ultrashort laser pulses, leading to their field-free, periodically recurring, highly squeezed, angular distributions (alignment), and serving as a preparation step for further interactions, such as strong field ionization [1] and dissociation, scattering off surfaces [2–4], deflection by inhomogeneous fields [5], high harmonic generation (HHG) [6–9], measurement of molecular frame photoelectron angular distributions [10,11], ultrafast x-ray diffraction (UXD) [12,13], and many others. However, the inversion symmetry of the interaction Hamiltonian for optical field-induced alignment preserves the up-down symmetry of the medium during and following the interaction, so no net orientation of asymmetric molecules is induced in the medium. Symmetry breaking and net molecular orientation has been achieved through the use of dc fields that interact with the molecular permanent electric dipole [14,15]. However, the presence of a dc field may affect the results of measurements performed on oriented samples and thus it is of special importance to achieve molecular orientation under field-free conditions, as was demonstrated recently through the use of moderate quasi-dc fields followed by pulsed optical excitation of low density, jet-cooled molecular samples [16–18]. Another approach used a two-color optical scheme in which the fundamental laser frequency was mixed with its second harmonic [19]. In these cases, however, the molecules are exposed to relatively

intense optical irradiation ($\sim 10^{13}$ W/cm^2) prior to their interrogation, potentially producing unwanted molecular excitation (which would be severe disadvantage for biological samples due to their relatively low damage thresholds).

In this work we demonstrate field-free orientation and alignment of polar gas-phase molecules by intense single-cycle THz fields at ambient conditions. We measure both the time-dependent orientation and alignment by probing the free-induction-decay (FID) and the transient birefringence induced by THz excitation. The measurements exploit recently achieved generation of THz pulses with microjoule energies [20,21], which has enabled nonlinear THz spectroscopy in solid [22–24], liquid [25], and now gas-phase samples.

Polar molecules can interact with EM fields that are resonant with their rotational transition frequencies via their permanent dipole moments. Classically, the linearly polarized field, $\vec{E}(t)$, acts to orient the initially isotropic molecular dipole vectors, $\vec{\mu}$, along the field direction through the interaction potential, $V(\theta, t) = -\vec{\mu} \cdot \vec{E}(t) = -\mu E(t) \cos(\theta)$, where θ is the angle between the field polarization and dipole vectors. This field exerts a torque on the molecules and initiates coherent rotational motion. Quantum mechanically, a resonant field couples adjacent opposite parity rotational states with $\Delta J = \pm 1$, $\Delta M = 0$, transferring population and inducing coherences that give rise to the emission of FID signals [26,27]. Excitation with a weak single-cycle THz pulse, the broad bandwidth of which includes many rotational transition frequencies, $2nBc$, where B is the molecular rotational constant (in cm^{-1}), c is the speed of light in vacuum, and $\{n\}$ are positive integers (i.e., a THz field, the single period of which is short compared to the associated rotational periods) produces coherences at all of the resonant transition frequencies [28,29]. Interferences among these single-quantum coherences suppress far-field emission, except when they all radiate in phase at equally spaced bursts termed "commensurate echoes", with a "revival" period of $T_{\rm rev} = 1/2Bc$. The far-field THz emission is detected at the times when the molecules undergoing coherent rotation

come into transient net orientation of their dipoles, as described by the ensemble average $\langle\langle\cos\theta\rangle\rangle$. This periodic behavior is closely reminiscent of the "quantum rotational revivals" [30–33] that follow nonresonant femtosecond optical excitation of two-quantum rotational coherences through impulsive stimulated rotational Raman scattering, also known as "laser induced molecular alignment."

In the present work we excite not just one-quantum rotational coherences but also multiple-quantum coherences through successive interactions between a strong THz field and the sample, and we detect, under field-free conditions, both the FID commensurate echoes observed earlier after weak THz excitation [28,29,34] and the alignment-induced birefringence previously observed only after intense optical excitation [32,33].

We used 6-mJ optical pulses to generate $\sim 4\,\mu J$ single-cycle THz pulses, as described previously [20,21]. About $2\,\mu J$ of the THz pulse energy reached the sample in a 10 cm long OCS gas cell at room temperature (the focusing parameters are found in the caption of Fig. 1). The transmitted THz field and the induced THz FID bursts or "commensurate echoes" that followed were measured by electro-optic sampling, i.e., through the birefringence that the THz field induced in a ZnTe nonlinear crystal, as monitored by a variably delayed optical readout pulse. The measured THz echoes revealed the induced molecular
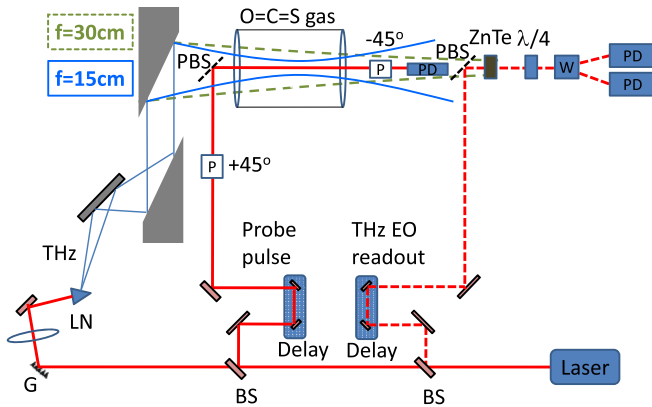

FIG. 1 (color online). Schematic representation of the two setups used in this work. An optical pulse was used to generate the single-cycle THz pulse that was passed through the gas cell to induce coherent rotational motion. Either the THz electro-optic (EO) readout pulse was generated for the measurement of the periodic FID emission owing to the induced molecular orientation, or the optical probe pulse was generated for measurement of the THz-induced birefringence due to molecular alignment. For the FID (birefringence) measurements the THz beam (FWHM ~ 1.5 cm) was focused by $f = 30$ cm ($f = 15$ cm) off axis parabolic reflectors to create the dashed green (solid blue) THz spatial distributions, respectively. G, grating; LN, lithium niobate THz generation crystal; BS, beam splitter; P, polarizer; W, Wollaston prism; PD, photodetector; PBS, Pellicle beam splitter. (In order to switch between the two setups, we replace the last parabolic reflector and remove the first Pellicle, the $-45°$ P and the single PD).

orientation, $\langle\langle\cos\theta\rangle\rangle(t)$. Alternatively, the induced molecular alignment, $\langle\langle\cos^2\theta\rangle\rangle(t)$, was determined by measurement of the induced birefringence in the gas, monitored by a variably delayed optical probe pulse.

Figure 2(a) depicts a THz pulse and the FID emission induced by it due to the orientation of OCS at 250 torr.

Following the intense THz pulse at $t = 0$, the data show signals at ~ 22 ps and ~ 30 ps due to reflections in the ZnTe crystal and the plastic (TOPAS, an amorphous, transparent copolymer) cell windows, respectively. The first three revivals are apparent at $T_{\mathrm{rev}} = 82$ ps intervals [marked as 1, 2, 3 in Fig. 2(a)].

Figure 2(b) shows the time-dependent birefringence due to THz-induced alignment in 350 torr OCS gas. The THz pulse was applied at time $t = 0$. The two peaks, located at ~ 1.3 ps and 0 ps, originate from both the instantaneous electronic response to the driving field, and the molecular alignment contributions to the birefringence (the latter is more pronounced at the second peak at $t = 1.3$ ps) and are in excellent agreement with our theoretical results. Strong revivals are observed at 41, 82, and 123 ps (1/2, 1, 3/2, T_{rev}, respectively) with inversion between successive signal profiles, a familiar feature of two-quantum rotational coherences [35,36]. Also apparent is an induced background signal level that reaches its maximum value at around the end of the THz pump pulse, $t \sim 2$ ps, and decays slowly thereafter. This background change is a manifestation of a nonthermal rotational state distribution owing to population transferred into higher rotational states, giving rise to a constant anisotropic angular distribution. Thus the total extent of alignment $\langle\langle\cos^2\theta\rangle\rangle(t)$ can be expressed as a sum of two parts, which are due to coherences $\langle\langle\cos^2\theta\rangle\rangle_c(t)$ and populations $\langle\langle\cos^2\theta\rangle\rangle_p(t)$ [37], both induced by two interactions with the THz field (which explains their relative amplitudes)

Figures 2(c) and 2(d) show the results of numerical simulations of time-dependent molecular orientation, $\langle\langle\cos\theta\rangle\rangle(t)$, and alignment, $\langle\langle\cos^2\theta\rangle\rangle(t)$, induced by a THz pulse with field profile, $E(t)$, consisting of a single sinusoidal or cosinusoidal cycle. In our calculations, we used the density matrix formalism and numerically solved the Liouville-Von Neumann equation, $\frac{\partial\rho}{\partial t} = -\frac{i}{\hbar}[H, \rho]$, where $H = \frac{\hat{L}^2}{2I} + V(\theta, t)$ is the Hamiltonian, $\hat{L}$ is the angular momentum operator, I is the moment of inertia, and $V(\theta, t) = -\mu E(t)\cos(\theta)$ is the interaction potential, as discussed above.

The calculated molecular orientation depicted in Fig. 2(c) shows the expected first recurrence, separated by the quantum revival time (T_{rev}). All of the subsequent recurrences at integer T_{rev} (not shown) are similar to the first. Note that the transient orientation profile at the first recurrence is 90° phase shifted with respect to the incident THz field profile. The FID profile [Fig. 2(a)] follows the gradient of the time-dependent macroscopic polarization (namely the orientation: the red curve in Fig. 2(c)] induced
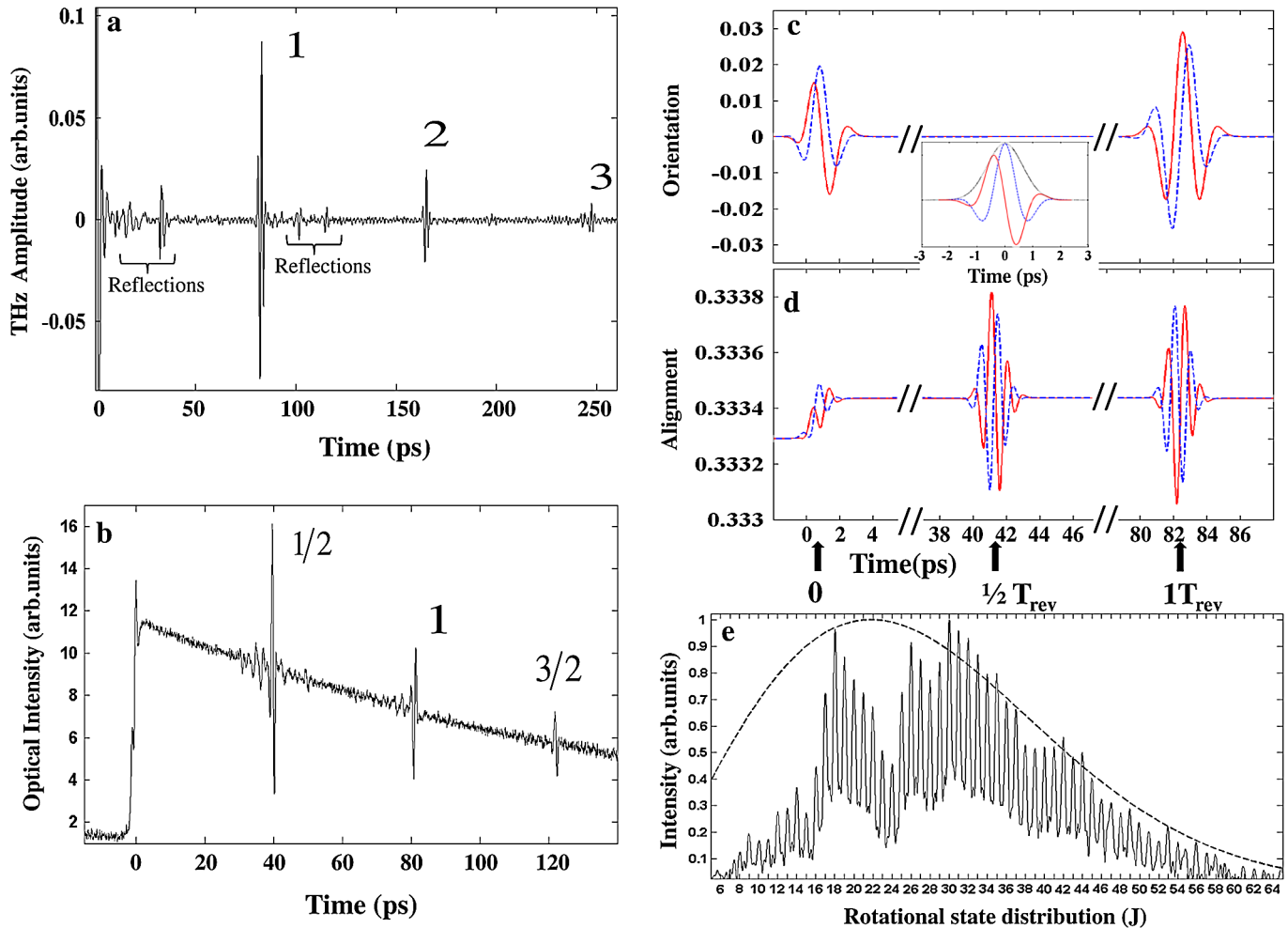
FIG. 2 (color online). (a) Electro-optic sampling of the FID emission from the OCS gas cell following the THz pulse. (b) Alignment-induced birefringence in 350 torr OCS at 300 K. (c) Numerical simulation results for orientation $\langle\langle\cos\theta\rangle\rangle(t)$ induced by a single-cycle THz pulse. Two simulations are shown for THz pulses with the same pulse envelope (inset, black dotted curve) and with fields phase-shifted by 90° (inset, solid red and dashed blue curves). (d) Numerical simulation results for alignment $\langle\langle\cos^2\theta\rangle\rangle(t)$ induced by a single-cycle THz pulse. Simulations are shown for the same phase-shifted THz waveforms as in (c) and for OCS gas at 300 K. (e) Normalized rotational level (J state) contribution to the coherent signal shown in (b). The calculated thermal rotational distribution at 300 K is depicted by the dashed curve.

in the medium as expected from Maxwell's equations. A 90° phase shift in the carrier-envelope phase (CEP) of the incident THz field (red vs blue) results in a corresponding phase shift in the induced orientation (and the THz field emitted by it). The calculated time-dependent molecular alignment, shown in Fig. 2(d), reveals recurrences separated by $T_{rev}/2$, indicating, in view of Fig. 2(c), that at half-revival times the sample shows orientationless alignment (thus retaining up-down symmetry), while at integer revival times the sample shows both net alignment and net orientation. Successive alignment profiles are inverted, and the 90° CEP shift in the driving field results in a 180° phase shift in the alignment profiles because it is induced by two interactions with the THz field. This marks an important difference between THz-induced and optically-induced molecular alignment, as the latter is CEP insensitive. The simulation also shows the steady-state background signal level due to the

THz-induced change in the J-state population distribution, however it does not include relaxation processes [37], which are outside the scope of the present Letter.

A Fourier transform of the time-domain alignment signal in Fig. 2(b) (after removal of the exponentially decaying background) yielded a succession of peaks at evenly spaced frequencies, which, when rescaled to the two-quantum rotational coherences ($f_{J,J+2} = (4J + 6)Bc$) of the OCS molecule $B = 0.203$ cm^{-1} [34], revealed the contributions of more than 50 rotational states to the observed signal, as shown in Fig. 2(e). Comparison to the initial thermal population (dashed line in Fig. 2(e)] shows that the THz pulse is sufficiently broad spectrally to induce coherences involving essentially all of the thermally populated rotational states.

Finally we estimate the magnitudes of the orientation and alignment that produced our detected signals. As has
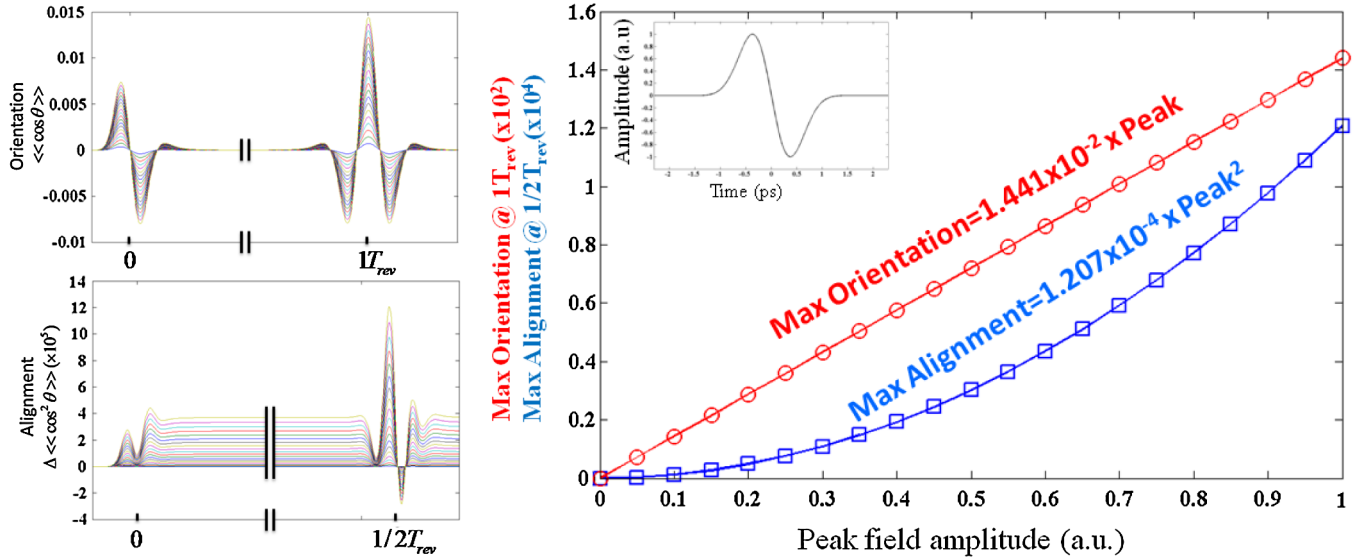
FIG. 3 (color online). (a) Time-dependent orientation and alignment induced in OCS at 300 K, calculated for a series of amplitudes of the driving field profile depicted in the inset of panel *b*. (b) By fitting the peak orientation and peak alignment we get their peak amplitude dependences on the driving field, as marked in the figure.

been discussed previously [37], the time-dependences of the two contributions to alignment, $\langle\langle\cos^2\theta\rangle\rangle_p(t)$ and $\langle\langle\cos^2\theta\rangle\rangle_c(t)$, can be approximated as single-exponential decays. We find the corresponding relaxation times to be $T_1 = 172$ ps and $T_2 = 57$ ps, and extrapolation to time $t = 0$ yields the amplitudes, $\langle\langle\cos^2\theta\rangle\rangle_p(0) = 11.6$ arb. units and $\langle\langle\cos^2\theta\rangle\rangle_c(0) = 25.7$ arb. units, for the data in Fig. 2(b), with the $\langle\langle\cos^2\theta\rangle\rangle_c(0)/\langle\langle\cos^2\theta\rangle\rangle_p(0) = 2.2$ ratio in good agreement with our numerical simulations.

The relation, $\frac{\Delta I}{I} = \sin(\frac{\Delta n \omega L}{c})$, correlates the observed signal level, $\frac{\Delta I}{I} = 9 \times 10^{-3}$, and the birefringence, Δn, induced in our experiment, yielding $\Delta n = 1.78 \times 10^{-8} = \frac{3N\Delta\alpha}{4n\varepsilon_0}\Delta\langle\langle\cos^2\theta\rangle\rangle$ [38], from which the maximal change in alignment factor is calculated to be $\Delta\langle\langle\cos^2\theta\rangle\rangle = 3.8 \times 10^{-5}$. In order to extract the degree of orientation induced, we used the degree of alignment determined experimentally, simulated the induced alignments and orientations at various field strengths, and correlated between the two observables as presented in Fig. 3. The results yielded a peak experimental orientation of 0.0086 ($\sim 1\%$) averaged over the cell. By measuring the THz field (amplitude and phase) throughout its propagation in the cell, we accounted for the intensity and CEP variations of almost $\pi/2$ due to the Gouy phase shift [39] over the interaction region. The theoretical analysis of the averaged alignment yielded a maximal orientation ~ 1.5 times higher near the focal plane, than the averaged value, namely, 1.3%. The averaged THz field amplitude found was ~ 22 kV/cm, which is 5–10 times smaller than our routinely generated peak fields [20] and far weaker than the ~ 1 MV/cm fields we can now generate and that have been reported recently [40]. Far higher degrees of alignment and orientation are expected with jet-cooled molecular samples and stronger (available) THz fields.

Intense single-cycle THz pulses have been used to induce field-free orientation and alignment in gas-phase polar molecules at room temperature. With realistic THz excitation conditions, optical measurements, such as HHG, x-ray diffraction, and ion-fragmentation imaging, can be performed on oriented samples and under field-free conditions. The combination of stronger THz fields (acting on the permanent dipole) and optical fields (acting on the anisotropic polarizabillity tensor) will offer two independent handles for controlling the 3D angular distribution of more complex (nonlinear polyatomic) molecules.

[1] I. V. Litvinyuk, Kevin F. Lee, P. W. Dooley, D. M. Rayner, D. M. Villeneuve, and P. B. Corkum, Phys. Rev. Lett. **90**, 233003 (2003).

[2] G. M. McClelland, G. D. Kubiak, H. G. Rennagel, and R. N. Zare, Phys. Rev. Lett. **46**, 831 (1981).

[3] B. G. Perkins Jr. and David J. Nesbitt, J. Phys. Chem. A **111**, 7420 (2007).

[4] Y. Khodorkovsky, I. Sh. Averbukh, and E. Pollak, J. Phys. Condens. Matter **22**, 304004 (2010).

[5] E. Gershnabel and I. Sh. Averbukh, Phys. Rev. Lett. **104**, 153001 (2010).

[6] R. Velotta, N. Hay, M. B. Mason, M. Castillejo, and J. P. Marangos, Phys. Rev. Lett. **87**, 183901 (2001).

[7] J. Itatani, J. Levesque, D. Zeidler, H. Niikura, H. Pepin, J. C. Kieffer, P. B. Corkum, and D. M. Villeneuve, Nature (London) **432**, 867 (2004).

[8] H. Soifer, P. Botheron, D. Shafir, A. Diner, O. Raz, B. D. Bruner, Y. Mairesse, B. Pons, and N. Dudovich, Phys. Rev. Lett. **105**, 143904 (2010).

[9] B. K. McFarland, J. P. Farrell, P. H. Bucksbaum, and M. Gühr, Science **322**, 1232 (2008).

[10] M. Meckel, D. Comtois, D. Zeidler, A. Staudte, D. Pavičić, H. C. Bandulet, H. Pépin, J. C. Kieffer, R. Dörner, D. M. Villeneuve, and P. B. Corkum, Science **320**, 1478 (2008).

[11] L. Holmegaard, J. L. Hansen, L. Kalhøj, S. L. Kragh, H. Stapelfeldt, F. Filsinger, J. Küpper, G. Meijer, D. Dimitrovski, M. Abu-samha, C. P. J. Martiny, and L. B. Madsen, Nature Phys. **6**, 428 (2010).

[12] J. Hajdu, Curr. Opin. Struct. Biol. **10**, 569 (2000).

[13] R. Neutze, R. Wouts, D. van der Spoel, E. Weckert, and J. Hajdu, Nature (London) **406**, 752 (2000).

[14] B. Friedrich and D. Herschbach, Nature (London) **353**, 412 (1991).

[15] B. Friedrich and D. Herschbach, J. Chem. Phys. **111**, 6157 (1999).

[16] L. Holmegaard, J. H. Nielsen, I. Nevo, H. Stapelfeldt, F. Filsinger, J. Küpper, and G. Meijer, Phys. Rev. Lett. **102**, 023001 (2009).

[17] A. Goban, S. Minemoto, and H. Sakai, Phys. Rev. Lett. **101**, 013001 (2008).

[18] O. Ghafur, A. Rouzée, A. Gijsbertsen, W. K. Siu, S. Stolte, and M. J. J. Vrakking, Nature Phys. **5**, 289 (2009).

[19] S. De, I. Znakovskaya, D. Ray, F. Anis, Nora G. Johnson, I. A. Bocharova, M. Magrakvelidze, B. D. Esry, C. L. Cocke, I. V. Litvinyuk, and M. F. Kling, Phys. Rev. Lett. **103**, 153002 (2009).

[20] K.-L. Yeh, M. C. Hoffmann, J. Hebling, and K. A. Nelson, Appl. Phys. Lett. **90**, 171121 (2007).

[21] K.-L. Yeh, J. Hebling, M. C. Hoffmann, and K. A. Nelson, Opt. Commun. **281**, 3567 (2008).

[22] M. Jewariya, M. Nagai, and K. Tanaka, Phys. Rev. Lett. **105**, 203003 (2010).

[23] J. Hebling, K.-L. Yeh, M. C. Hoffmann, and K. A. Nelson, IEEE J. Sel. Top. Quantum Electron. **14**, 345 (2008).

[24] M. C. Hoffmann, J. Hebling, H. Y. Hwang, K.-L. Yeh, and K. A. Nelson, J. Opt. Soc. Am. B **26**, A29 (2009).

[25] M. C. Hoffmann, N. C. Brandt, H. Y. Hwang, K.-L. Yeh, and K. A. Nelson, Appl. Phys. Lett. **95**, 231105 (2009).

[26] K. Prozument, A. P. Colombo, Y. Zhou, G. B. Park, V. S. Petrovic, S. L. Coy, and R. W. Field, Phys. Rev. Lett. **107**, 143001 (2011).

[27] G. B. Park, A. H. Steeves, K. Kuyanov-Prozument, J. L. Neill, and R. W. Field, J. Chem. Phys. **135**, 024202 (2011).

[28] H. Harde, S. Keiding, and D. Grischkowsky, Phys. Rev. Lett. **66**, 1834 (1991).

[29] H. Harde and D. Grischkowsky, J. Opt. Soc. Am. B **8**, 1642 (1991).

[30] P. M. Felker, J. S. Baskin, and A. H. Zewail, J. Phys. Chem. **90**, 724 (1986).

[31] I. Sh. Averbukh and N. F. Perelman, Phys. Lett. A **139**, 449 (1989).

[32] T. Seideman, Phys. Rev. Lett. **83**, 4971 (1999).

[33] H. Stapelfeldt and T. Seideman, Rev. Mod. Phys. **75**, 543 (2003).

[34] D. Bigourd, G. Mouret, A. Cuisset, F. Hindle, E. Fertein, and R. Bocquet, Opt. Commun. **281**, 3111 (2008).

[35] S. Fleischer, I. Sh. Averbukh, and Y. Prior, Phys. Rev. A **74**, 041403 (2006).

[36] S. Fleischer, I. Sh. Averbukh, and Y. Prior, Phys. Rev. Lett. **99**, 093002 (2007).

[37] S. Ramakrishna and T. Seideman, Phys. Rev. Lett. **95**, 113001 (2005).

[38] B. Lavorel, O. Faucher, M. Morgen, and R. Chaux, J. Raman Spectrosc. **31**, 77 (2000).

[39] A. B. Ruffin, J. V. Rudd, J. F. Whitaker, S. Feng, and H. G. Winful, Phys. Rev. Lett. **83**, 3410 (1999).

[40] H. Hirori, F. Blanchard, and K. Tanaka, Appl. Phys. Lett. **98**, 091106 (2011).